X-761-74-23

PREPRINT

NASA TM X- 70671

TEMPERATURE, ILLUMINATION AND FLUENCE DEPENDENCE OF CURRENT AND VOLTAGE IN ELECTRON IRRADIATED SOLAR CELLS

A.F. OBENSCHAIN

T.J. FAITH

DECEMBER 1973

GSFC

GODDARD SPACE FLIGHT CENTER

GREENBELT, MARYLAND

X-761-74-23
PREPRINT

TEMPERATURE, ILLUMINATION AND FLUENCE DEPENDENCE OF CURRENT AND VOLTAGE IN ELECTRON IRRADIATED SOLAR CELLS*

A. F. Obenschain
NASA/GSFC

T. J. Faith
RCA/AED
Princeton, N.J.

December 1973

*This work was supported by NASA/GSFC Contract NAS 5-21642

ABSTRACT

Emperical equations have been derived from measurements of solar cell photovoltaic characteristics relating light-generated current, I_L, and open circuit voltage, V_o, to cell temperature, T, intensity of illumination, W, and 1 Mev electron fluence, ϕ. Both 2 ohm-cm and 10 ohm-cm cells were tested over the ranges: $123^oK \leqslant T \leqslant 473^oK$, $5\ mW/cm^2 \leqslant W \leqslant 1830\ mW/cm^2$ and $1 \times 10^{13}\ e/cm^2 \leqslant \phi \leqslant 1 \times 10^{16}\ e/cm^2$.

The temperature dependency of I_L is similar for both resistivities at 140 mW/cm^2; at high temperature ($T \geqslant 273^oK$) the temperature coefficient varies with fluence as $\phi^{0.18}$, while at low temperatures the coefficient is relatively independent of fluence. Fluence-dependent degration causes a decrease in I_L at a rate proportional to $\phi^{0.153}$ for both resistivities. At all intensities other than 560 mW/cm^2, a linear dependence of I_L on illumination was found. Open circuit voltage equations were derived for all temperatures except 123^oK and 173^oK, where Schottky barrier effects and cell shunting led to questionable experimental results. The temperature coefficient of voltage was, to a good approximation, independent of both temperature and illumination for both resistivities. Illumination dependence of V_{oc} was logarithmic (the voltage increasing by approximately 0.025 V and 0.032 V per decade increase in illumination for 10 ohm-cm and 2 ohm-cm cells respectively), while the decrease with fluence of V_{oc} varied as $\phi^{0.25}$ for both resistivities.

CONTENTS

ILLUSTRATIONS

ILLUSTRATIONS (Continued)

TEMPERATURE, ILLUMINATION AND FLUENCE DEPENDENCE OF CURRENT AND VOLTAGE IN ELECTRON IRRADIATED SOLAR CELLS

I. INTRODUCTION

Utilization of solar cells as the primary power source for spacecraft missions ranging from approximately Mercury orbit to Jupiter orbit has received wide consideration. Sun oriented solar panels experience illumination intensities greater than 1000 mW/cm^2 and temperatures greater than $473^{o}K$ in Mercury orbit and only 5 mW/cm^2 at temperatures ranging down to approximately $130^{o}K$ in Jupiter orbit. Many works have been published on cell behavior at both the high[1,2] and low[3-7] extremes of this illumination/temperature range, and an extensive body of data exists on electron irradiated cells in the middle ranges, i.e., for earth-orbit conditions.[8] The purpose of the present work was to cover the entire temperature/illumination range with the same set of electron irradiated n/p cells with two different base resistivities. This report presents results of measurements of light-generated current and open-circuit voltage and of an analysis of these measurements which led to empirical equations enabling easy comparisons between the two cell resistivities.

A more complete discussion, including I-V curve fits is available elsewhere,[9] and in recent work to be published.

II. EXPERIMENTAL PROCEDURE

The solar cells used in these experiments were 1 cm X 2 cm commercial grade n/p silicon cells with Ti-Ag solderless contacts, manufactured by Centralab. Two different base resistivities were tested, pre-irradiation capacitance measurements on several cells indicating values of approximately 10 ohm-cm and 2 ohm-cm. Five cells of each resistivity were irradiated at room temperature by 1 MeV electrons from a Van de Graaf generator to one of the following fluences: 0, 1×10^{13}, 3×10^{13}, 1×10^{14}, 3×10^{14}, 1×10^{15}, 3×10^{15}, or 1×10^{16} e/cm^2. Post irradiation measurements were made on all cells at 50°K temperature increments over the temperature range from 123°K to 473°K. Cell illumination at intensities of 5, 35, 140, 560 and 1830 mW/cm^2 was provided by an Aerospace Controls Corporation model 302 xenon arc solar simulator. The temperature/illumination matrix for cell measurements is shown in Figure 1. The cells, which were soldered to a copper-plated kovar cell block bolted to a vacuum cold finger, were held within ±2°K of the nominal measurement temperature by the proper combination of liquid nitrogen in the cold finger and electrical power to a heater coil attached to the cell block. Five test cells plus a dummy cell carrying a copper-constantan thermocouple were mounted on each cell block, the data to be presented representing values averaged over the

five cells. Photovoltaic current-voltage characteristics were generated automatically by a Spectrolab model D550 electronic load and displayed on a Mosely model 7030 A X-Y recorder. Open-circuit voltage and short-circuit current were displayed on a NLS model 3020 digital voltmeter, the voltmeter being shunted by an SRI precision 1 ohm resistor for current display. Cell temperature was measured using a Rubicon model 2745 potentiometer in conjunction with the copper-constantan thermocouple soldered to the dummy cell.

A 3-inch diameter, 1/4-inch thick Corning 7940 fused silica disc with flat optical transmission from 0.4 μm to 1.2 μm provided a sight glass for cell illumination inside the vacuum cold finger vessel. Calibration of the intensity of illumination was provided by a standard cell calibrated at Table Mountain, Ca. which was mounted beside the cell block location, 3 inches from the center of the block, and in the same test plane. The intensity of illumination at the test plane was varied by adjusting either the xenon arc current or the distance between the arc and the test plane. Low intensity illumination (5 and 35 mW/cm^2) was accomplished using a set of neutral density filters purchased for Aerospace Controls Corporation. To establish high intensity, W, the standard cell was centered on the beam axis and a filter combination with transmission equal to 140 mW/cm^2 was placed in the beam. Xenon arc current and distance were adjusted to yield a standard cell current of 63.1 mA. Removal of the filters then established the illumination intensity at W. Since the test cells view the illuminator through a sight glass, a companion sight glass was placed in front

of the standard to equalize the transmission to the standard and the test cells. The standard cell temperature was maintained at 30°C using a circulating brine system.

The experimental error in the measurement of I_L varies from ±1.4 percent for cells of either resistivity where $W \leq 140$ mW/cm^2, $T \geq 273$°K, and $\phi < 1 \times 10^{15}$ e/cm^2, to ±3.6 percent for $W > 140$ mW/cm^2, $T < 273$°K, $\phi \geq 1 \times 10^{15}$ e/cm^2 and 2 ohm-cm cell resistivity. The combined uncertainty in the measurement of V_o is estimated to be approximately ±0.012 V.[9]

III. RESULTS AND ANALYSIS

Light-Generated Current

Results of measurements of light-generated current, I_L, are shown in Figures 2 to 9 where I_L is plotted versus temperature with fluence a parameter. Figures 2 and 3 show results for 10 Ω-cm and 2 Ω-cm cells, respectively, at an illumination intensity of 140 mW/cm^2. Figures 4 and 5 and Figures 6 and 7 show equivalent results for intensities of 35 mW/cm^2 and 560 mW/cm^2, respectively, while Figures 8 and 9 give results for both resistivities at 5 mW/cm^2 and 1830 mW/cm^2, respectively. The solid lines in these figures represent empirical equations for I_L developed in the manner outlined below.

The analysis was initiated at the center of the temperature illumination matrix, 273°K and 140 mW/cm^2. Light-generated current

$I_L(4, 3, \phi)$* was plotted versus fluence and empirical fits were established. A good fit to the experimental data, with a single equation valid over the entire fluence range, was obtained using a power law dependence of current on fluence:

for 10 Ω-cm cells:

$$I_L(4, 3, \phi) = 81.7 - 0.134\phi^{0.153} \tag{1}$$

for 2 Ω-cm cells:

$$I_L(4, 3, \phi) = 83.6 - 0.154\phi^{0.153} \tag{2}$$

both of which apply over the entire fluence range from 1×10^{13} e/cm^2 to 1×10^{16} e/cm^2 (but not for $\phi = 0$). Figures 10 and 11 show the curves representing equations (1) and (2), respectively, together with the appropriate experimental data. One large (3.6 percent) deviation between equation (2) and the data appears at $\phi = 1 \times 10^{14}$ e/cm^2. This has been tentatively ascribed to the particular cells measured at this fluence, which displayed unusual behavior in temperature cycling.

The temperature dependence of I_L under 140 mW/cm^2 illumination was next considered. For temperatures of 273°K and above the light-generated current varied approximately linearly with temperature with a temperature

*$I_L = I_L(T, W, \phi)$ with T, W, and ϕ being represented by integers n.

T: (n = 1 to 8) representing T = 73 + 50n (°K)

W: (n = 1 to 5) representing W = 5, 35, 140, 560, and 1830 mW/cm^2

ϕ: (n = 1 to 7) representing $\phi \approx 10^{(n + 25)/2}$ (e/cm^2).

Thus $I_L(4, 3, \phi)$ refers to T = 273°K, W = 140 mW/cm^2.

coefficient that increased with increasing fluence. It was found that the temperature coefficient, dI_L/dT, divided by the current at 273°K, $I_L(4, 3, \phi)$, followed a power law relationship with fluence. This relationship is seen in Figure 12 which gives plots of normalized temperature coefficient versus fluence. Both 10 Ω-cm and 2 Ω-cm cell data are fitted to a good approximation by the relationship,

$$\frac{1}{I_L(4,3,\phi)} \frac{dI_L}{dT} = 3.23 \times 10^{-6} \phi^{0.18} \tag{3}$$

over the entire fluence range.

At temperatures below approximately 223°K the behavior was different, the temperature coefficient being relatively independent of fluence. This was particularly true for the 10 Ω-cm cells where dI_L/dT averaged 0.055 mA/°K. For 2 Ω-cm cells a slight fluence dependence was apparent, but a large scatter in the data prompted the use of the value averaged over all fluences, which was 0.062 mA/°K.

Combining the temperature and fluence dependencies, equations can be written for the light-generated current valid for all temperatures and fluences covered in the experiment. The current is given by

$$I_L(T,3,\phi) = I_L(4,3,\phi)\left[1 + \frac{1}{I_L(4,3,\phi)} \frac{dI_L}{dT} (T - 273)\right] \tag{4}$$

For 10 Ω-cm cells, for $T \geqslant 223^{\circ}K$:

$$I_L(T, 3, \phi) = (81.7 - 0.134\phi^{0.153})[1 + 3.23 \times 10^{-6}\phi^{0.18}(T - 273)] \quad (5)$$

and for $T \leqslant 223^{\circ}K$:

$$I_L(T, 3, \phi) = I(3, 3, \phi) + 0.055(T - 223) \quad (6)$$

where $I(3, 3, \phi)$ is obtained from equation (10);

for 2 Ω-cm cells, for $T \geqslant 273^{\circ}K$:

$$I_L(T, 3, \phi) = (83.6 - 0.154\phi^{0.153})[1 + 3.23 \times 10^{-6}\phi^{0.18}(T - 273)] \quad (7)$$

and for $T \leqslant 273^{\circ}K$:

$$I_L(T, 3, \phi) = 83.6 - 0.154\phi^{0.153} + 0.062(T - 273) \quad (8)$$

Note that in equation (5), the high temperature equation for 10 Ω-cm cells extends to a lower temperature than its counterpart for 2 Ω-cm cells, equation (7). As a consequence the low temperature equation (6) is based on $I_L(3, 3, \phi)$, the current at $223^{\circ}K$, rather than $I_L(4, 3, \phi)$, the current at $273^{\circ}K$.

Several characteristics which the two resistivities have in common are clear from the data and the similarities in their empirical equations. One which shows up in Figures 2 and 3 is the match between high and low temperature coefficients at low fluence, i.e., the linearity of I_L vs T over the entire

temperature range. However, several subtle but significant differences are in evidence. First, as noted above, the high temperature equation for the 10 Ω-cm cells extends down to 223°K, 50°K further than its counterpart for 2 Ω-cm cells. Secondly, although there is an obvious break in the curves for $\phi \geq 3 \times 10^{14}$ e/cm^2 for both resistivities, the break is significantly stronger for the 10 Ω-cm cells, their temperature coefficient being lower at low temperature and higher at high temperature than that for the 2 Ω-cm cells. (The normalized temperature coefficients, equation (3), are the same for both resistivities at high temperature, but the normalizing currents are lower for the 2 Ω-cm cells. Consequently, the absolute coefficients are higher for the 10 Ω-cm cells.)

In deriving empirical equations for illumination intensities other than 140 mW/cm^2, the initial approach assumed the fluence and temperature dependencies obtained at 140 mW/cm^2 and a linear dependence of current on illumination, i.e.,

$$I_L(T, W, \phi) = \frac{W}{140} I_L(T, 3, \phi) \tag{9}$$

where $I_L(T, 3, \phi)$ is obtained from the appropriate number among equations (5) through (8).

Figure 4 indicates that equation (9) provides a good fit to the 10 Ω-cm data, predicting the break in the slope (temperature coefficient) which is in evidence in the data. In corresponding plots for 2 Ω-cm cells in Figure 5, the

break in the slope is not in evidence in the data. Since no data was taken at 35 mW/cm^2 above 323°K, (50°K above the break for 2 Ω-cm cells at 140 mW/cm^2 illumination) it is not possible to ascertain from the present data whether or not this break is actually absent in the 2 Ω-cm cells.

All of the data at 5 mW/cm^2 (Figure 8) are at 223°K and below so equations (6) and (8), the low-temperature equations which give fluence-independent temperature coefficients, apply. This fluence-independence is reflected in the data for cells of both resistivities.

Equation (9) did not fit the data at 560 mW/cm^2 so a modification was made by replacing the factor W/140 in this equation by ξ_W where ξ_W is an illumination-dependent coefficient determined separately for each cell resistivity but is independent of fluence and cell temperature. This drops the assumption of a linear current-illumination relationship but maintains the temperature and fluence relationships derived for 140 mW/cm^2 illumination. The criterion for the best-fit value of ξ_W was that the deviation between the equation and the data averaged over the 35 data points be zero. This resulted in values for ξ_W of 3.66 and 3.63 for 10 Ω-cm cells and 2 Ω-cm cells, respectively. These values are approximately 9 percent below the value of 4.0 for W/140. The reason for this apparent divergence from linearity is not known. However, other workers have observed linear current-illumination relationships to higher intensities than those measured here. Thus it is tentatively concluded that a calibration error

due to uncertainties in neutral-density filter transmission is responsible for the apparent non-linearity.

The curves in Figure 9 represent ξ_W values of 12.86 and 12.50 for 10 Ω-cm cells and 2 Ω-cm cells, respectively. These values are within 5 percent of the value of 13.1 for W/140. Considering the experimental error of up to ±4 percent at 1830 mW/cm^2 and cell-to-cell variations of up to 10 percent at this intensity, this difference is not considered significant. The equations give adequate predictions of fluence dependence, and the predicted increase in temperature coefficient with fluence is in evidence at both 560 mW/cm^2 and 1830 mW/cm^2. However, given the high degree of scatter in the experimental results at these intensities, the criteria for an equation describing them are rather modest, i.e., a reasonably good general fit and a form proven valid in other experiments with a better data base.

An indication of the quality of the empirical fit to the data was obtained by computing the percent deviation, E, given by

$$E = 100 \frac{(I_D - I_E)}{(I_D + I_E)/2} \tag{10}$$

where I_D and I_E are the values of light-generated current obtained from the experimental data and from the appropriate empirical equation, respectively.

For 10 Ω-cm cells, all but 3 of the 55 points for W = 140 mW/cm^2 show a deviation between data and equation of less than three percent, only one point

shows a deviation greater than 4 percent, the point at $\phi = 1 \times 10^{16}$ e/cm^2, T = 473°K, which is 8.3 percent higher than the equation predicts. Examination of Figures 2 and 3 shows an upturn in data at 473°K at other fluences as well as at 1×10^{16} e/cm^2 suggesting a greater than linear increase in current at very high temperatures. Close examination of the data indicates the possibility of further complexities in temperature dependence. Such complexities have been previously reported,[10] however, the equations derived here are believed to be adequate given the experimental accuracy of the present results.

At other illuminations the number of points representing greater than 4 percent deviation are: 3 of 34 points for 35 mW/cm^2, 5 of 35 points for 560 mW/cm^2, 5 of 20 points for 5 mW/cm^2, 4 of 20 points for 1830 mW/cm^2. The quality of the fit is thus best at 140 mW/cm^2 and is worst at the ends of the illumination matrix, i.e., at 5 and 1830 mW/cm^2. For 2 Ω-cm cells, the number of points representing greater than 4 percent deviation are: 3 of 56 points for 140 mW/cm^2, 4 of 35 points for 35 mW/cm^2, 7 of 34 points for 560 mW/cm^2, 7 of 21 points for 5 mW/cm^2, and 3 of 19 points for 1830 mW/cm^2.

Open-Circuit Voltage

Plots of open-circuit voltage versus cell temperature with illumination as a parameter are given in Figures 13 to 16, Figures 13 and 14 for 10 Ω-cm and 2 Ω-cm cells, respectively for $\phi = 3 \times 10^{14}$ e/cm^2 and Figures 15 and 16 for $\phi = 1 \times 10^{16}$ e/cm^2. This data, together with those at other fluences was fitted

in a manner similar to that employed for light-generated current. The resulting equations are, for 10 Ω-cm cells,

$$V_o(T, W, \phi) = 0.621 - 9.35 \times 10^{-6}\ \phi^{0.25} - 0.0023(T - 273) + 0.025 \ln\left(\frac{W}{140}\right) \quad (11)$$

and for 2 Ω-cm cells,

$$V_o(T, W, \phi) = (0.651 - 9.35 \times 10^{-6}\ \phi^{0.25}) - C_T(T - 273) + 0.032 \ln\left(\frac{W}{140}\right) \quad (12)$$

where C_T = 0.0022 V/°K for $1 \times 10^{13} \leqslant \phi \leqslant 1 \times 10^{14}$ e/cm^2, and 0.0023 V/°K for $3 \times 10^{14} \leqslant \phi \leqslant 1 \times 10^{16}$ e/cm^2. As suggested by equation (11), the temperature coefficient for 10 Ω-cm cells was to a good approximation independent of both temperature and fluence. In contrast, the temperature coefficient for 2 Ω-cm cells has a significant fluence dependence as described by these two different values of C_T. In addition, the coefficient of the illumination-dependent term is larger for the 2 Ω-cm cells. Otherwise the equations are very similar; in particular for W = 140 mW/cm^2 and $\phi \geqslant 3 \times 10^{14}$ e/cm^2 the difference in open-circuit voltage between the two resistivities is constant at 0.030 V.

An interesting feature in the data for both resistivities is the approximate parallelism in the curves at different illuminations, reflected in the illumination-dependent terms of equations (11) and (12). The diode equation gives:

$$V_o = \frac{AkT}{e} \ln\left[\frac{I_L - I_o}{I_o}\right] \quad (13)$$

where e is the electron charge, k is Boltzmann's constant and I_L is the reverse saturation current. For an ideal diode A = 1; for actual solar cells a summation of terms, each having different values of A and I_o is often used to fit the experimental curves. For temperatures near room temperature the portion of the curve near V_o usually fits the ideal diode well.[11] Under such circumstances the difference in V_o, ΔV_o, between two illuminations W_1 and W_2 is proportional to cell temperature,

$$\Delta V_o = \frac{AkT}{e} \ln \left(\frac{W_2}{W_1} \right) \tag{14}$$

However, the data and equations (11) and (12) show V_o to be relatively independent of temperature. This corresponds to an A factor in equation (14) that is inversely proportional to cell temperature. An inverse temperature dependence of A has previously been suggested by Barrett et al[12] based on low temperature measurements by Kennerud.[13] In interpreting the present results as implying such a temperature dependence, a stipulation must be made, i.e., the measurements cover different illuminations in different temperature ranges. Thus it would be improper to use equation (11) or (12) for T/W combinations not measured, e.g., 432°K/35 mW/cm^2 or 273°K/560 mW/cm^2. In addition, the validity of the equations is limited to the temperature range above 223°K. Below this temperature evidence of both Schottky barrier formation and cell shunting invalidated open-circuit voltage data.

The experimental uncertainty of the measurements was essentially constant at ±0.012 V. Therefore, the quality of the empirical fit was tested by calculating the difference between data and equation directly in volts. For 10 Ω-cm cells the fits to all data points at 5, 35, and 560 mW/cm^2 are within the experimental uncertainty of the measurements. At 140 mW/cm^2 one reading differs from the equation by 0.017 V, the equation giving the higher value. However, this data point was at 223°K, where Schottky barrier effects begin to reduce V_o. Similarly at 1830 mW/cm^2 one reading differs from the equation by 0.017 V, the equation value being lower. The fits for 2 Ω-cm cells are not as good as those for the 10 Ω-cm cells. The number of readings for which the empirical voltage equation differs from the corresponding experimental point by more than 0.012 V are: 3 of 42 points for 35 mW/cm^2, 8 of 34 points for 560 mW/cm^2, and 4 of 21 points for 1830 mW/cm^3. In spite of some rather significant divergences, it is felt that both the current and voltage equations provide a valid (and certainly convenient) basis for a first approximation comparisons between cell resistivities.

IV. CONCLUSIONS

Photovoltaic characteristics have been measured on solar cells irradiated with 1 Mev electrons to fluences ranging from 1×10^{13} e/cm^2 to 1×10^{16} e/cm^2, for cell temperatures ranging from 123°K to 473°K and illumination intensities ranging from 5 mW/cm^2 to 1830 mW/cm^2. Emperical equations have been

derived from these measurements to describe the behavior of light-generated current and open circuit voltage over various portions of these temperature/illumination ranges. Both 10 Ω-cm and 2 Ω-cm n/p silicon solar cells were tested, similar analytical expressions being sought to provide a basis for easy comparisons between the two resistivities.

Equations for light-generated current were obtained for both resistivities covering the entire experimental T/W range. The temperature dependencies are similar for both resistivities—at high temperature ($T \geqslant 273^{o}K$) the normalized temperature coefficient varies with fluence as $\phi^{0.16}$; at low temperature the coefficient is relatively independent of fluence. A power law relationship was generated for fluence dependence at $273^{o}K$; at this temperature it was determined that light-generated current decreased at a rate proportional to $\phi^{0.153}$ for both resistivities. The coefficient of the power law expression was larger for 2 Ω-cm cells, consequently the advantage in current for 10 Ω-cm cells increased with increasing fluence.

Open circuit voltage equations have been derived for all temperatures except $123^{o}K$ and $173^{o}K$, where Schottky barrier effects and cell (high A factor) shunting led to questionable experimental results. The temperature coefficient of voltage was, to a reasonable approximation, independent of temperature and illumination for both resistivities and for 10 Ω-cm cells was 0.0023 $V/^{o}K$ independent of fluence. For 2 Ω-cm cells it was 0.0022 $V/^{o}K$ for low fluences and 0.0023 $V/^{o}K$ for fluences of 3×10^{14} e/cm^2 and above. Illumination dependence

was logarithmic, the voltage increasing by approximately 0.025 V and 0.032 V per decade increase in illumination for 10 Ω-cm cell and 2 Ω-cm cells, respectively. At T = 273°K, the decrease with fluence varied at $\phi^{0.25}$ for both resistivities. At 140 mW/cm^2 the voltage difference between 2 and 10 Ω-cm cells, as given by equations, is constant at 0.030 V (independent of temperature) for $\phi \geq 3 \times 10^{14}$ e/cm^2. Since the illumination dependence is stronger in the 2 Ω-cm cells, this 0.030 V advantage increases at high intensity and decreases at low intensity.

In deriving analytical equations to fit the data the principal guidelines were to generate the minimum number of equations compatible with an acceptably good fit, as dictated by uncertainties and scatter in the raw data. Since the data was the most coherent near the center of the temperature/illumination matrix (273°K, 140 mW/cm^2), the results here show the best correspondence between the raw data and those calculated from the derived equations; the spread increases at the extremes of the matrix, so the quality of the fit is not as good in these regions. It is felt, however, that a good start at characterizing solar cell performance over the specified fluence, temperature and illumination ranges has been made.

ACKNOWLEDGEMENT

The writers wish to acknowledge the encouragement and support of Dr. D. W. Harris of NASA-GSFC and of P. Nekrasov of RCA. T. Glock, R. Neadle, and W. Rutan provided capable support in the design and fabrication of experimental apparatus and in the performance of measurements. P. Pierce, now at EOS, collaborated in the early stages of the program. Cell irradiations were performed by J. Groppe of RCA Laboratories.

REFERENCES

1. C. A. Lewis and J. P. Kirkpatrick, Conf. Record of Eighth Photovoltaic Spec. Conf., IEEE catalog No. 70C 32 ED, 123 (1970).

2. P. A. Iles, Final Report, JPL Contract No. 952865, issued by Centralab Div. of Globe - Union Inc., Nov. 30, 1971.

3. H. W. Brandhorst and R. E. Hart, Conf. Record of Eighth Photovoltaic Spec. Conf., IEEE catalog No. 70C 32 ED, 142 (1970).

4. J. C. Ho, F. T. C. Bartels, and A. R. Kirkpatrick, Conf. Record of Eighth Photovoltaic Spec. Conf., IEEE catalog No. 70C 32 ED, 150 (1970).

5. W. Luft, Conf. Record of Eighth Photovoltaic Spec. Conf. IEEE catalog No. 70C 32 ED, 161 (1970).

6. P. A. Payne and E. L. Ralph, Conf. Record of Eighth Photovoltaic Spec. Conf. IEEE catalog No. 70C 32 ED, 135 (1970).

7. N. D. Wilsey and R. J. Lambert, Conf. Record of Eighth Photovoltaic Spec. Conf. IEEE catalog No. 70C 32 ED, 169 (1970).

8. J. H. Martin, R. L. Statler, and E. L. Ralph, Second Intersociety Energy Conversion Engineering Conf. Proc., 289 (1970).

9. T. J. Faith, Final Report, NASA Contract No. NAS5-21642, issued by RCA, April 1973.

10. E. L. Ralph, Conf. Record of Sixth Photovoltaic Spec. Conf., IEEE catalog No. 15C53 Volume I, 98 (1967).

11. M. Wolf and H. Rauschenbach, Adv. Energy Conversion, 3, 455 (1963).

12. M. J. Barrett, M. B. Hornstein and R. H. Stroud, Final Report, JPL Contract No. 952548, prepared by Exotech Inc., June 15, 1970.

13. K. L. Kennerud, IEEE Trans. on Aerospace and Electronic Systems, AES-3, 586 (July 1967).

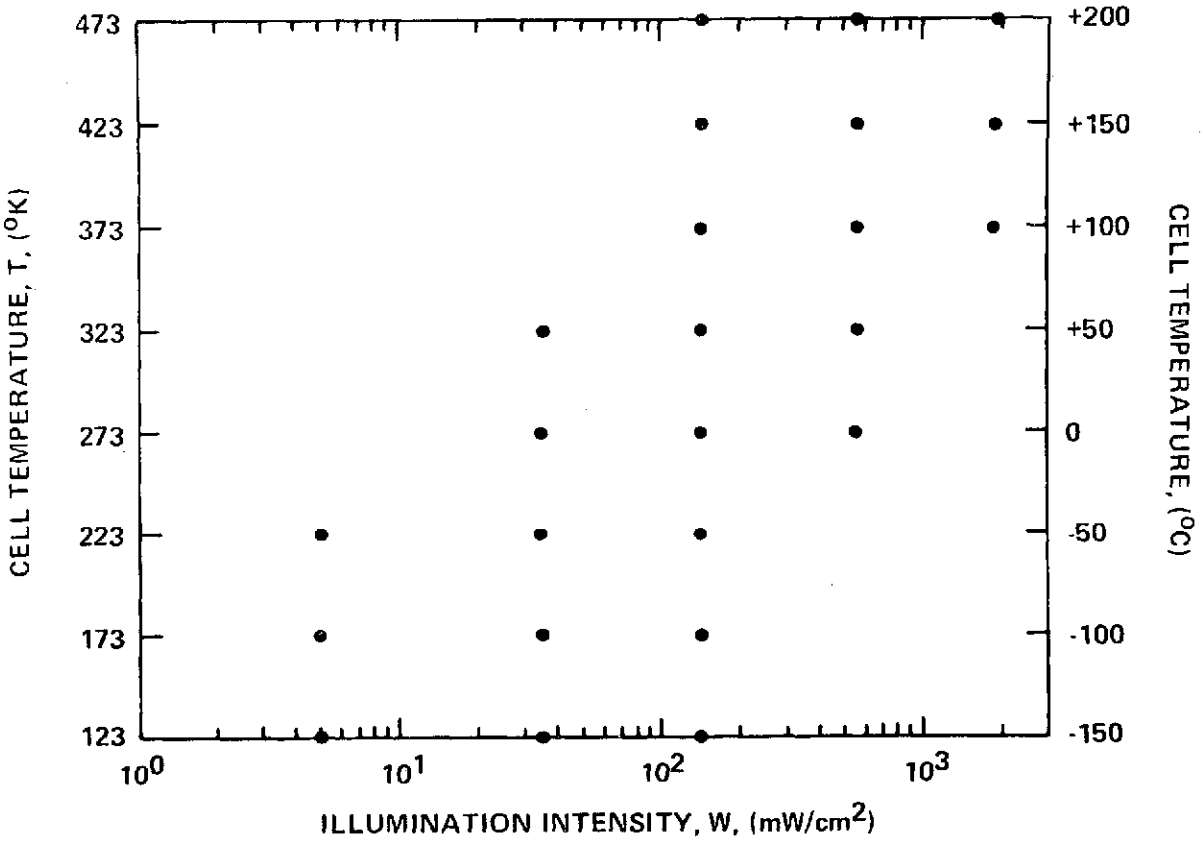

Figure 1. Temperature-Illumination Combinations at Which Cells Were Measured

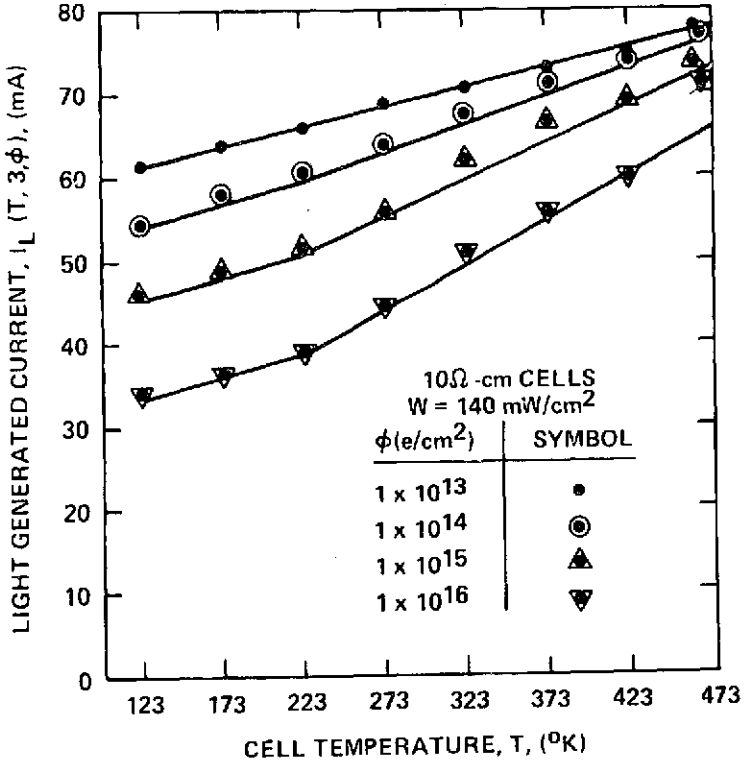

Figure 2. Light Generated Current at W = 140 mW/cm^2 Versus Cell Temperature and Fluence, 10 Ω-cm Cells

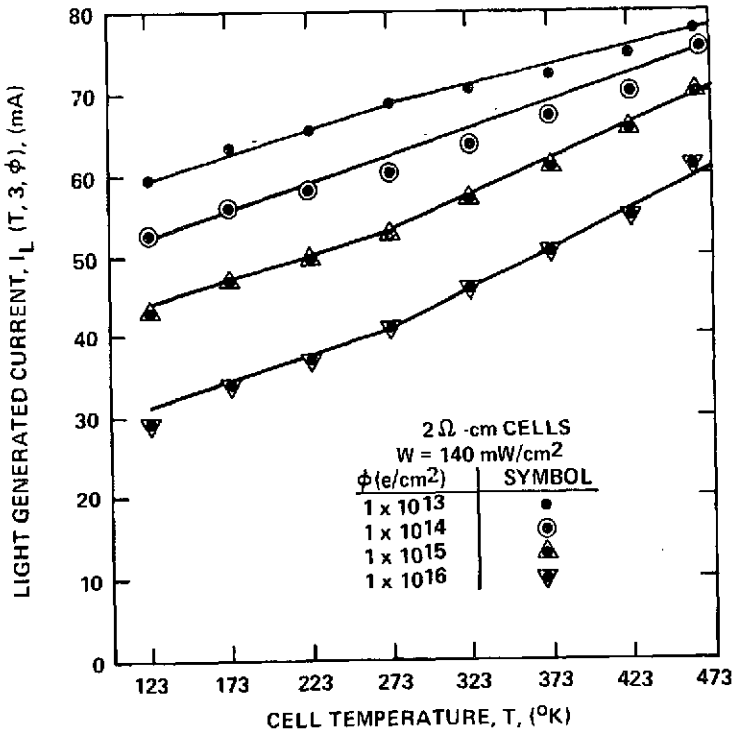

Figure 3. Light Generated Current at W = 140 mW/cm^2 Versus Cell Temperature and Fluence, 2 Ω-cm Cells

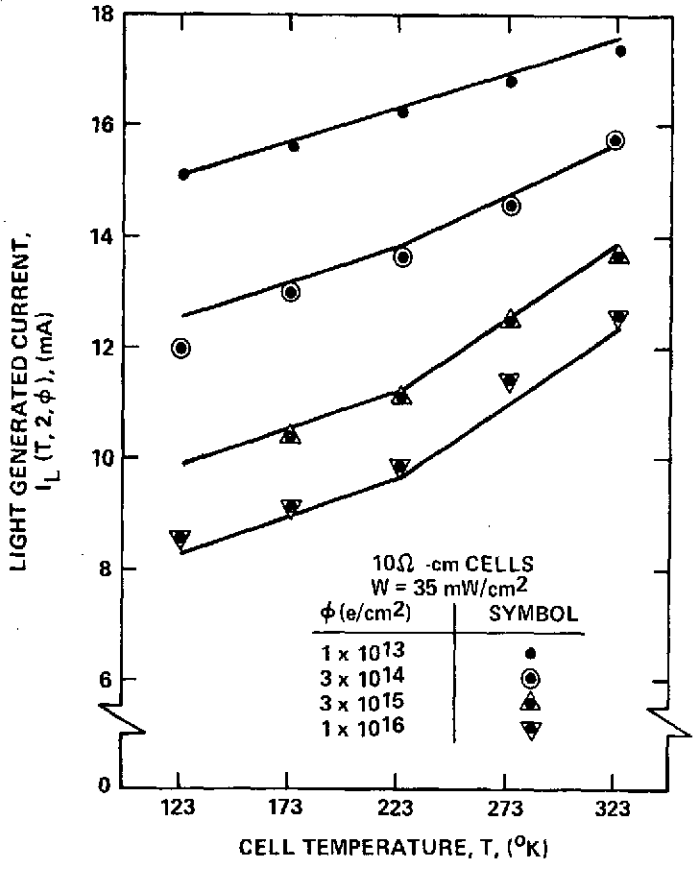

Figure 4. Light Generated Current at W = 35 mW/cm^2 Versus Cell Temperature and Fluence, 10 Ω-cm Cells

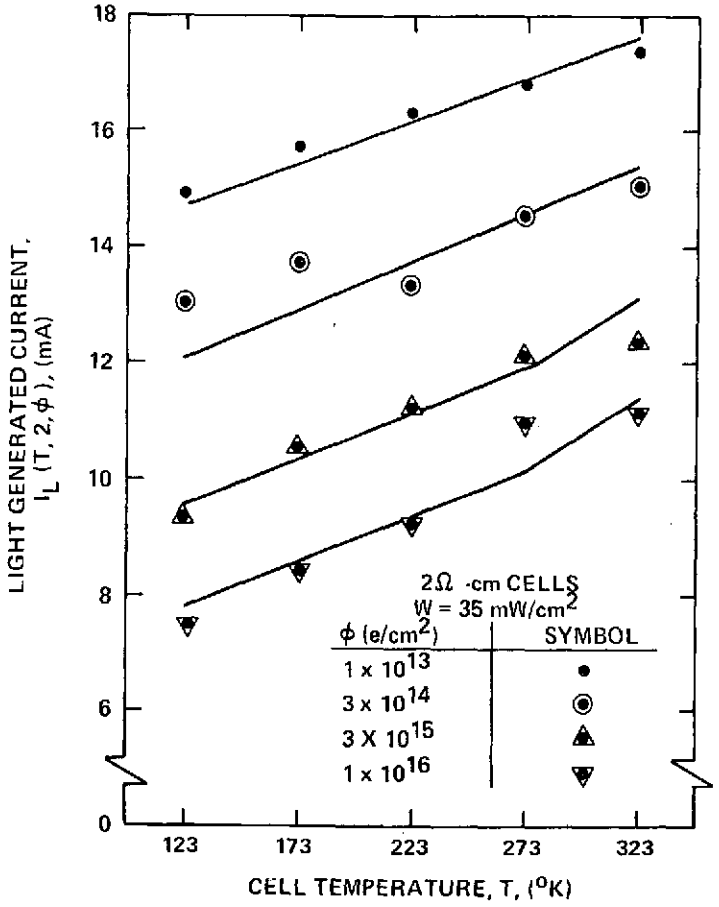

Figure 5. Light Generated Current at W = 35 mW/cm^2 Versus Cell Temperature and Fluence, 2 Ω-cm Cells

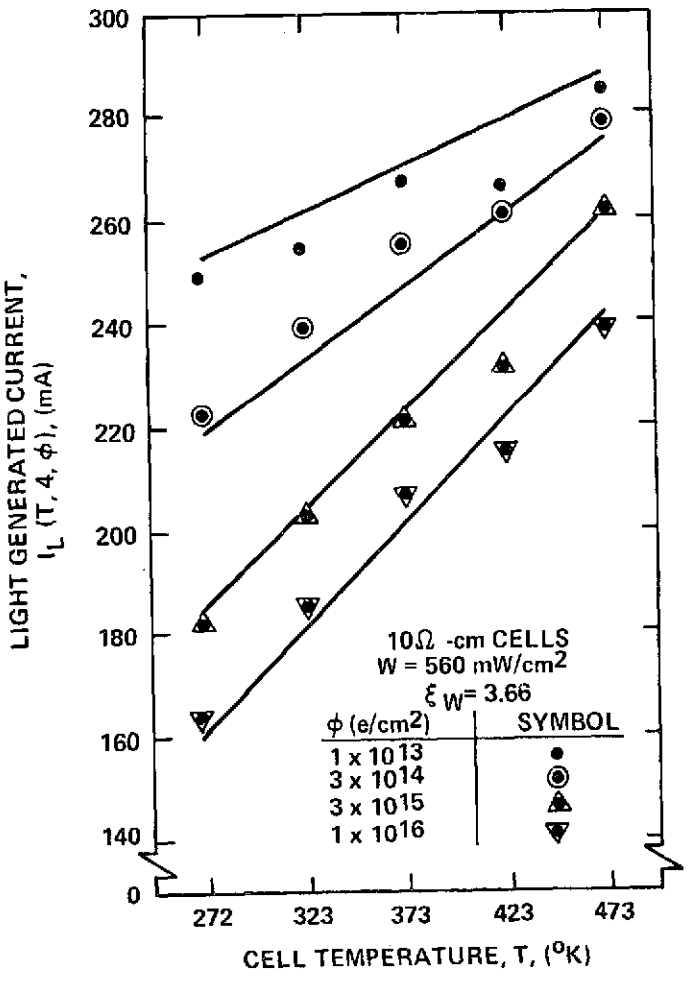

Figure 6. Light Generated Current at W = 560 mW/cm^2 Versus Cell Temperature and Fluence, 10 Ω-cm Cells

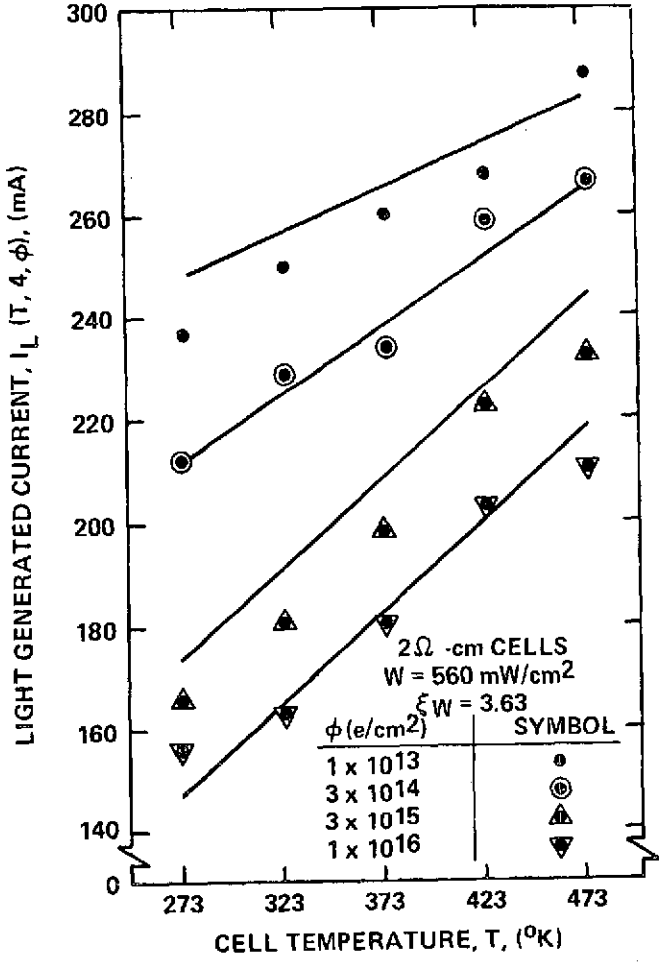

Figure 7. Light Generated Current at W = 560 mW/cm^2 Versus Cell Temperature and Fluence, 2 Ω-cm Cells

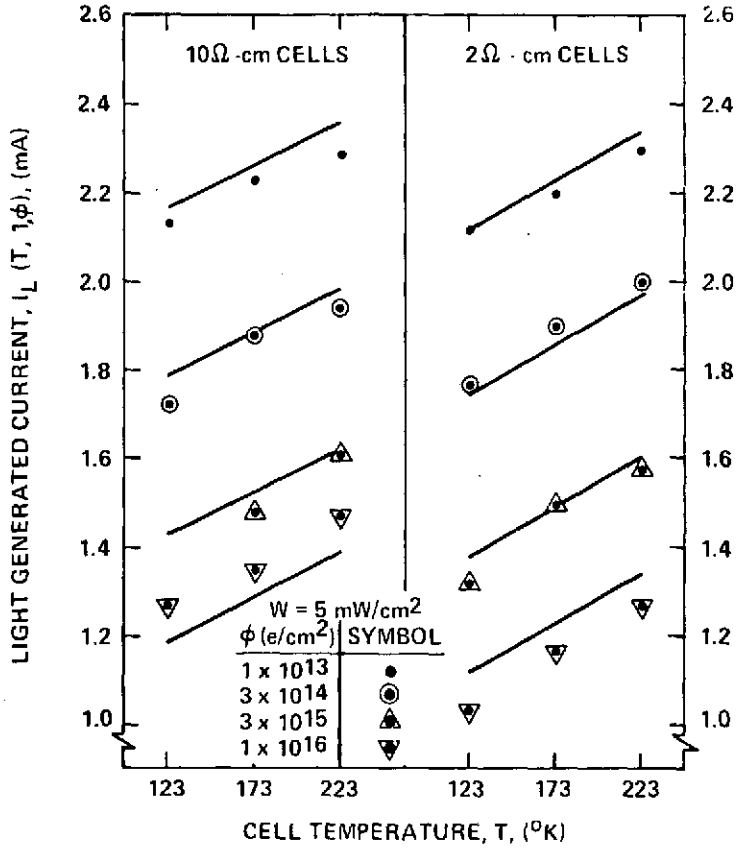

Figure 8. Light Generated Current at W = 5 mW/cm^2 Versus Cell Temperature and Fluence, 10 Ω-cm and 2 Ω-cm Cells

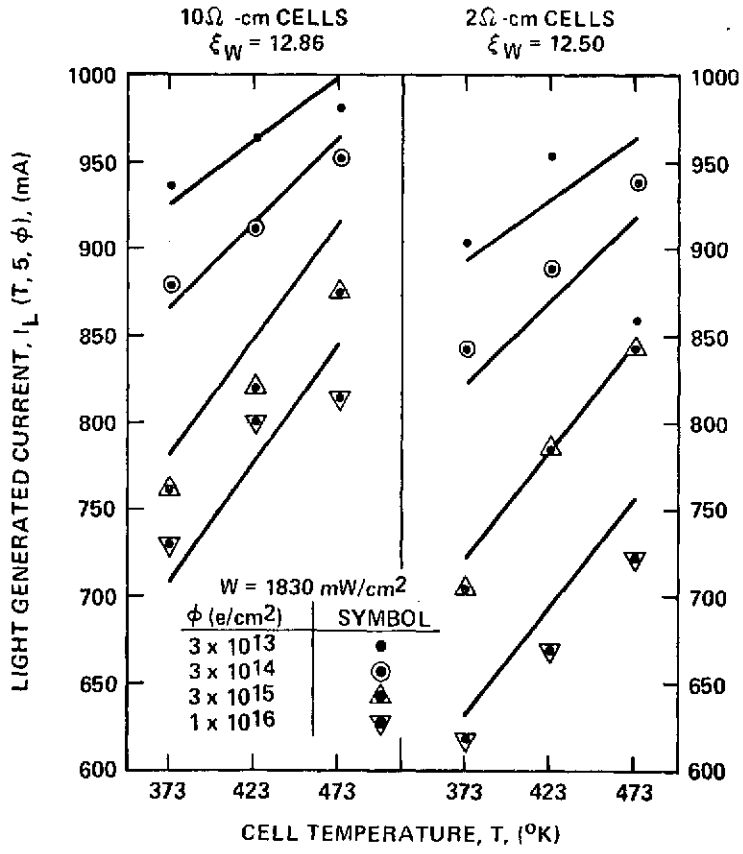

Figure 9. Light Generated Current at W = 1830 mW/cm^2 Versus Cell Temperature and Fluence, 10 Ω-cm and 2 Ω-cm Cells

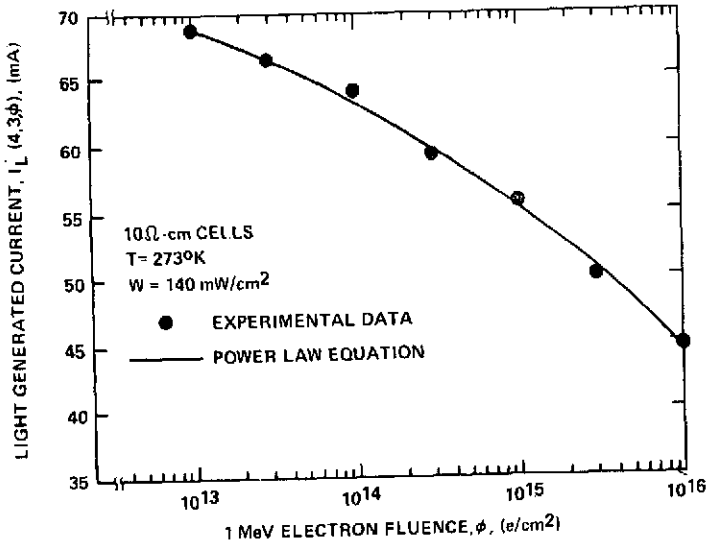

Figure 10. Light Generated Current Versus Fluence at 273°K and 140 mW/cm² Illumination, 10 Ω-cm Cells

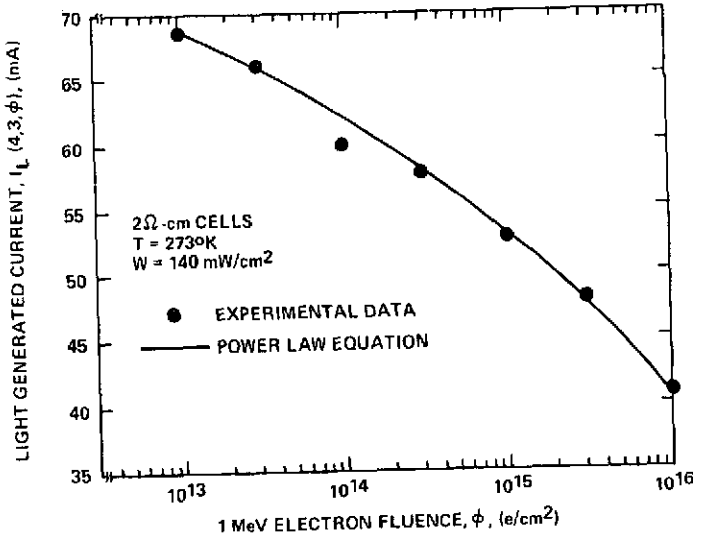

Figure 11. Light Generated Current Versus Fluence at 273°K and 140 mW/cm² Illumination, 2 Ω-cm Cells

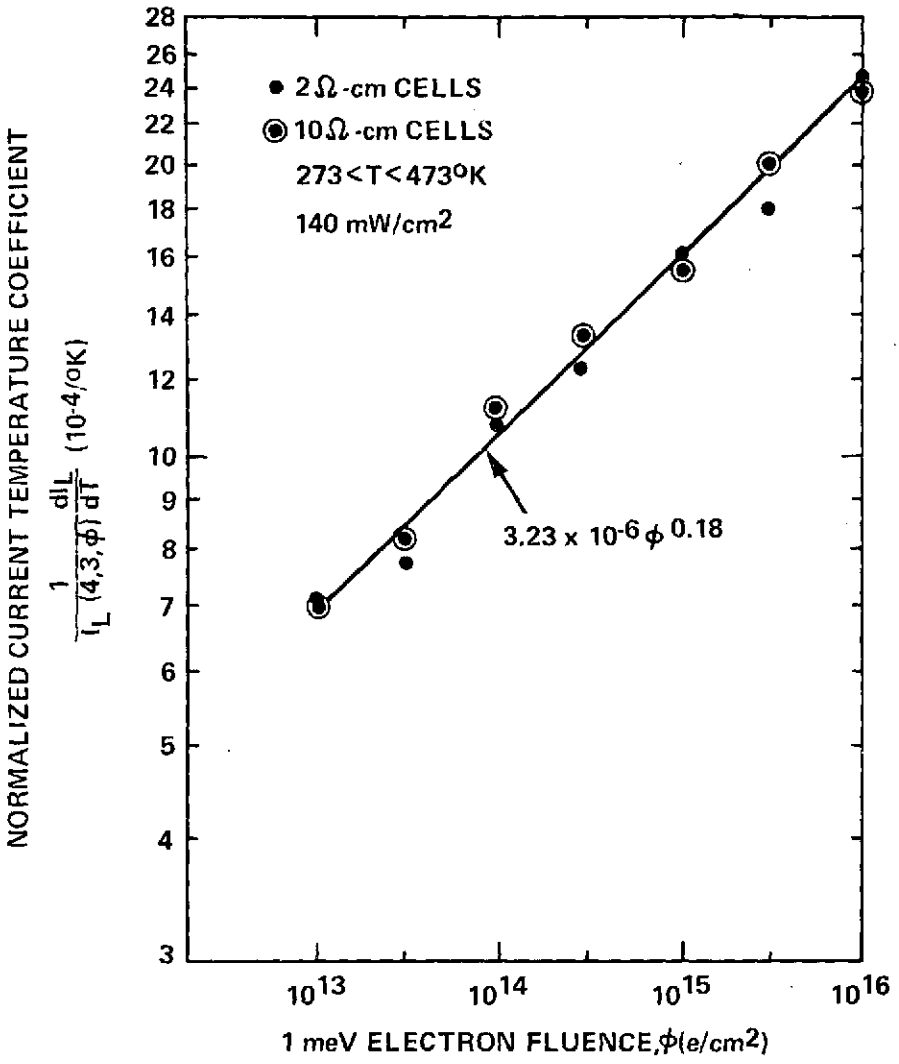

Figure 12. Normalized Temperature Coefficient of Light Generated Current Versus Fluence

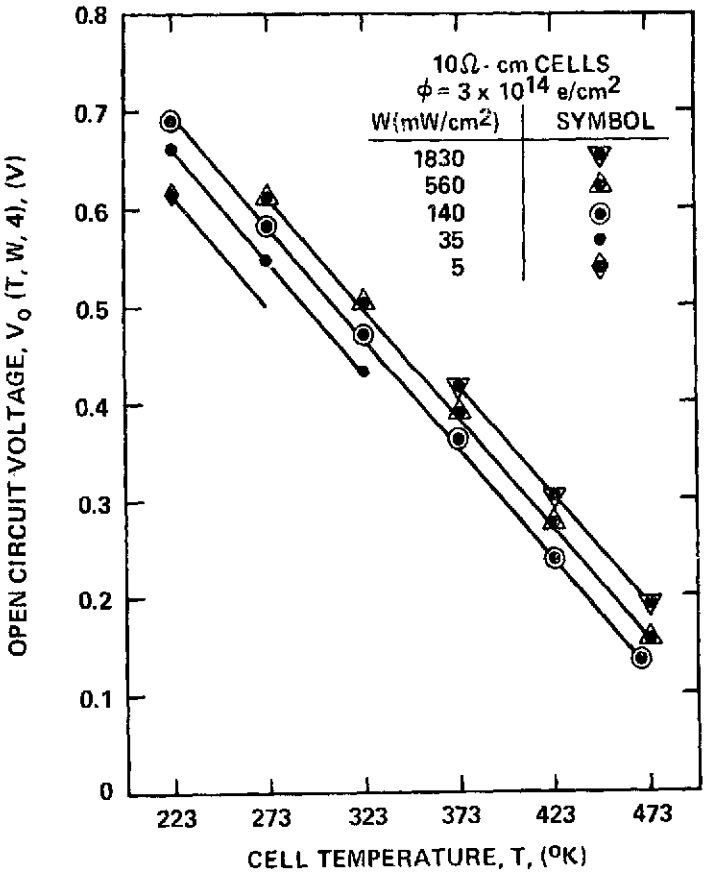

Figure 13. Open Circuit Voltage Versus Cell Temperature and Illumination at $\phi = 3 \times 10^{14}$ e/cm^2, 10 Ω-cm Cells

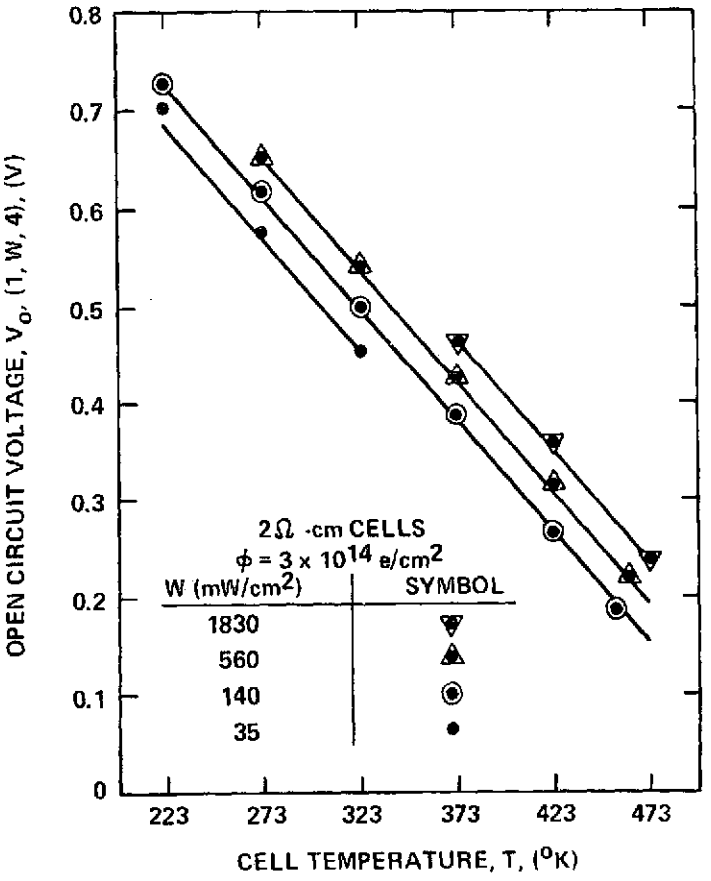

Figure 14. Open Circuit Voltage Versus Cell Temperature and Illumination at $\phi = 3 \times 10^{14}$ e/cm^2, 2 Ω-cm Cells

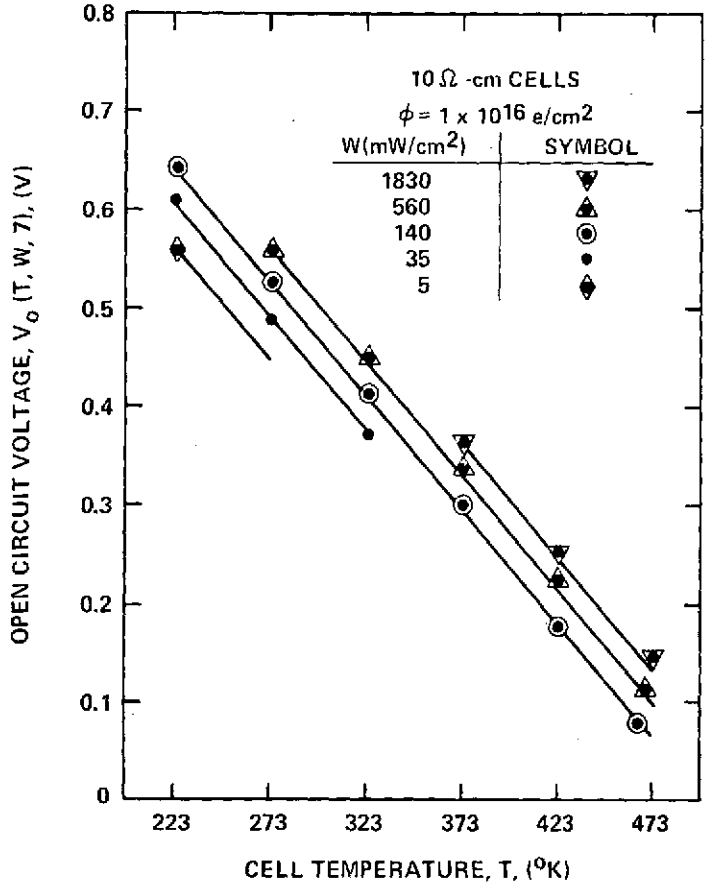

Figure 15. Open Circuit Voltage Versus Cell Temperature and Illumination at $\phi = 1 \times 10^{16}$ e/cm^2, 10 Ω-cm Cells

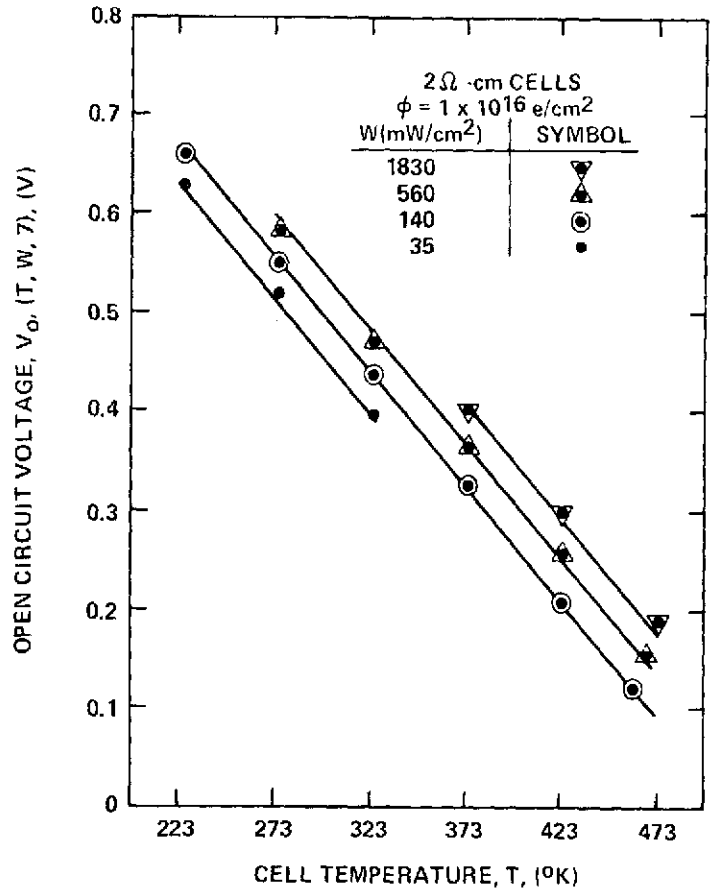

Figure 16. Open Circuit Voltage Versus Cell Temperature and Illumination at $\phi = 1 \times 10^{16}$ e/cm^2, 2 Ω-cm Cells